Available online at www.sciencedirect.com
SCIENCE DIRECT
International Journal of Mass Spectrometry 245 (2005) 61–67
International Journal of Mass Spectrometry
www.elsevier.com/locate/ijms

Photocatalytic degradation of methylene blue on nanocrystalline TiO_2: Surface mass spectrometry of reaction intermediates

Hubert Gnaser [a,*], Michael R. Savina [b], Wallis F. Calaway [b], C. Emil Tripa [b], Igor V. Veryovkin [b], Michael J. Pellin [b]

[a] *Department of Physics, University of Kaiserslautern, D-67663 Kaiserslautern, Germany*
[b] *Materials Science Division, Argonne National Laboratory, Argonne, IL 60439, USA*

Received 25 May 2005; received in revised form 13 July 2005; accepted 13 July 2005
Available online 11 August 2005

Abstract

Photocatalytic degradation reactions of methylene blue on nanocrystalline TiO_2 (nc-TiO_2) films were studied in situ by surface mass spectrometric techniques including secondary ion mass spectrometry, laser desorption direct ion mass spectrometry, and laser desorption/laser photoion mass spectrometry. The parent ion of methylene blue and/or its reduced form leucomethylene blue was observed with little fragmentation by all methods prior to ultraviolet exposure. The surface composition changed upon ultraviolet (UV) irradiation in air, an observation ascribed to photocatalytic reactions induced by UV photons: the parent molecule signal diminished and intermediate reaction products such as sulfoxides and sulfones were detected from the TiO_2 surface. After prolonged UV irradiation these species also vanished and the methylene blue appeared to be almost completely mineralized.

Keywords: Photocatalysis; Nanocrystalline TiO_2; Surface mass spectrometry; Methylene blue

1. Introduction

Nanocrystalline TiO_2 (nc-TiO_2) has attracted great interest in recent years due to its many potential applications [1–5]. Among these, the photocatalytic properties of nc-TiO_2 clearly stand out: to degrade organic or biological pollutants in waste water or in the atmosphere constitutes a very promising application [6–8]. Numerous studies [9–13] have investigated ultraviolet (UV) photocatalytic degradation reactions employing nc-TiO_2 particles in aqueous suspensions. The underlying physico-chemical mechanisms appear to be clear cut [14–16]: TiO_2 in the anatase phase (which exhibits the higher photocatalytic efficiency) is a semiconductor with a band gap of $E_g \sim 3.2$ eV. A UV photon with an energy greater than E_g creates an electron–hole pair in a TiO_2 nanocrystallite. If these charge carriers diffuse to the crystallite surface before recombining, they may reduce or oxidize adsorbed molecular species. The ultimate goal would be the complete mineralization of any pollutants present. While many studies have demonstrated the feasibility of that approach, detailed reaction pathways could be established only in a very limited number of cases. To some extent, this is due to the fact that most of those investigations were carried out in solution. Under such conditions, the assessment of the reaction processes occurring on the surface of the nc-TiO_2 particles is rather restricted.

It is generally assumed that the absorption of photons with an energy $h\nu \geq E_g = 3.2$ eV induces the following reactions at the surface of nc-TiO_2:

Electron–hole pair formation:

$$TiO_2 + h\nu \rightarrow TiO_2\,(e^- + h^+) \quad (1)$$

Oxidation of adsorbed water by holes:

$$(H_2O)_{ads} + h^+ \rightarrow H^+ + OH^\bullet \quad (2)$$

* Corresponding author. Tel.: +49 631 2054038; fax: +49 631 2052854.
E-mail address: gnaser@rhrk.uni-kl.de (H. Gnaser).

1387-3806/$ – see front matter © 2005 Elsevier B.V. All rights reserved.
doi:10.1016/j.ijms.2005.07.003

Ionosorption of adsorbed oxygen by electrons:

$$(O_2)_{ads} + e^- \rightarrow O_2^{\bullet -} \quad (3)$$

Oxidation of adsorbed hydroxide ions by holes:

$$2(OH^-)_{ads} + h^+ \rightarrow OH^- + OH^{\bullet} \quad (4)$$

Transient formation of hydroperoxide radicals via Eq. (3) and the further reactions:

$$O_2^{\bullet -} + H^+ \rightarrow HOO^{\bullet} \quad (5)$$

$$2HOO^{\bullet} \rightarrow H_2O_2 + O_2 \quad (6)$$

$$H_2O_2 + e^- \rightarrow OH^- + OH^{\bullet} \quad (7)$$

Oxidation of organics by $OH^{\bullet}$ radicals, or directly by holes:

$$R{-}H + OH^{\bullet} \rightarrow R^{\bullet} + H_2O \quad (8)$$

$$R + h^+ \rightarrow R^{+\bullet} \rightarrow \text{degradation products} \quad (9)$$

The goal of this work was to use mass spectrometry of desorbed surface species to monitor photocatalytic reactions such as those initiated by Eqs. (8) and (9) and followed by insertion of oxygen occurring on the surface of nc-TiO_2 particles. Such reactions have been studied in suspensions containing nc-TiO_2 particles, but in many applications, nc-TiO_2 is used in the form of films supported on substrates [17]. Hence, a direct probe of photocatalytic processes occurring on the nc-TiO_2 via mass spectrometry of desorbed surface species is desirable. In such techniques, atomic and molecular species are desorbed by means of ion or laser beams and detected either directly as ions or as neutrals upon a suitable post-ionization step [18]. Methylene blue (MB), a common organic dye, was studied because of its ubiquitous use and because the removal of dyes from waste waters constitutes an acute problem [19]. Furthermore, extensive research into the degradation of methylene blue [20–24] and of many other dyes [25–35] in aqueous nc-TiO_2 suspensions has already been performed. In the present work, films treated with MB were analyzed before and after UV exposure, and intermediate species in the photocatalytic reaction pathway were detected.

2. Experimental

2.1. Preparation of TiO_2 films

Nanocrystalline TiO_2 particles (anatase phase, of either 6, 12, or 20 nm particles) were suspended in an ethanol/water mixture and deposited on glass substrates by spin coating. Calcination at 500 °C for 1 h resulted in stoichiometric TiO_2 films composed of nanocrystallites with an average size identical to the original powder material, as determined by X-ray diffraction and transmission electron microscopy [36,37]. Methylene blue (chloride) was dissolved in methanol (120 mg/L) and a single drop was applied onto the surface spreading over the ~30 mm^2 nc-TiO_2 films.

Both pristine and UV-exposed films were investigated by mass spectrometry. The UV exposures were done in air by means of a xenon–mercury arc lamp (λ = ~250–380 nm).

2.2. Mass spectrometry

Most of the mass spectra were obtained using the CHARISMA time-of-flight mass spectrometer, which has been described in detail elsewhere [38,39]. Two means of desorbing and ionizing material from the nc-TiO_2 surface were used. A pulsed Nd:YAG laser operating in the third harmonic mode (λ = 355 nm, pulse width = 8 ns) focused to a ~90 μm × 150 μm elliptical spot (60° incidence) was used to desorb and ionize material in what are referred to as direct ion spectra. Secondary ion mass spectra (SIMS) were collected by bombarding the surface with either a 5 kV Ar^+ beam (900 ns pulse, 250 nA, ~1 mm spot size, 60° incidence) or a 15 kV Ga^+ beam (200 ns pulse, 20 nA, 10 μm spot, 60° incidence). Repetition rates were 500 Hz for the laser desorption and 1 kHz for the ion beams.

In addition, mass spectra were obtained using the SPIRIT instrument, which has been described in detail elsewhere [40]. This instrument is similar to CHARISMA except that the ion extraction optics are more efficient and the desorption laser is a nitrogen laser (λ = 337 nm, pulse width = 10 ns, 6 μm spot size, normal incidence). Owing to a lower pulse energy, the N_2 laser did not directly ionize the desorbed species as the Nd:YAG laser did, rather the desorbed neutrals were post-ionized with a F_2 laser (λ = 157 nm, 10 ns pulse width).

3. Results and discussion

The objectives of the present work are: (i) to explore the optimal mass spectrometric approach to study photocatalytic reactions on the surface of nanocrystalline TiO_2 films, (ii) to follow changes in the molecular composition on the TiO_2 surface induced by UV irradiation and thereby derive information about photocatalytic reactions, and (iii) to determine whether the laser photons responsible for desorption in the mass spectrometer might affect the analysis by themselves inducing photodegradation reactions.

3.1. Mass spectrometry of methylene blue on TiO_2 films

The 5 kV Ar^+ SIMS spectrum of MB on nc-TiO_2 is shown in Fig. 1. The 15 kV Ga^+ SIMS spectrum was nearly identical. In addition to a large number of low-mass peaks due either to fragmentation or organic contamination, we observe strong peaks corresponding to the MB cation at m/z = 284 (structure a in Fig. 2). However, the manifold of peaks in the parent ion region shows excesses at m/z = 285 and 286 that are not attributable to the isotopomers of MB. Whereas the expected

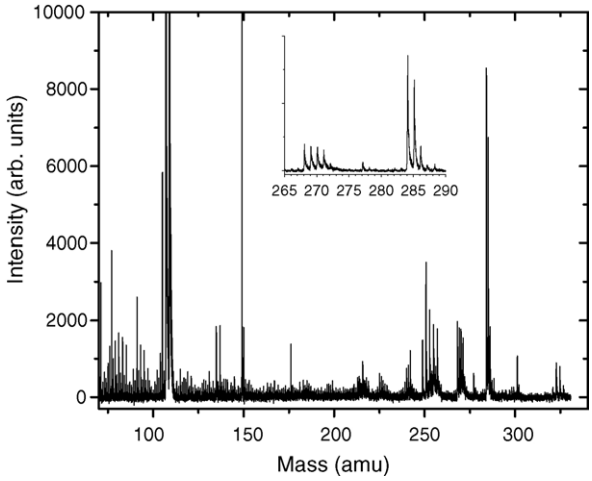

Fig. 1. Secondary ion mass spectrum (5 keV Ar^+) of methylene blue on a nc-TiO_2 film.

ratio of intensities of the peaks at 284, 285, and 286 due to MB alone is 1/0.2/0.06, the observed ratio is 1/0.83/0.22, indicating that a significant amount of signal in the $m/z = 284$ manifold (∼40%) is due to $[MB + H]^+$. The structure of the $m/z = 285$ ionic moiety is not known, however its neutral precursor is likely to be leucomethylene blue (LMB, structure b in Fig. 2), the reduced form of methylene blue. Whether the LMB was initially present on the surface or was formed as a result of the Ar^+ bombardment is not known.

The SIMS spectrum also shows manifolds of peaks due to $[MB–(CH_2)_n]^+$, corresponding to replacement of methyl groups with protons. These are likely due to fragmentation of the parent ion to produce the well-known homologues of MB such as Azure B (270 amu), Azure A (256 amu), and Azure C (240 amu). Unlike the parent, these species show strong peaks at $[M-1]^+$ and $[M-2]^+$.

In contrast to the SIMS spectrum, the laser desorption direct ion mass spectrum shows $[LMB]^+$ as the dominant peak, with only a very minor amount of $[MB]^+$ present (Fig. 3). The $m/z = 285$ peak manifold has the expected isotopomer distribution for LMB, and the ratio of LMB to MB is ∼9:1. The homologue peaks (Azure A and Azure B) also have the $[M+H]^+$ ions as the dominant species. As in the SIMS spectrum, the $[M]^+$, $[M-1]^+$, and $[M-2]^+$ peaks of Azure A and B are also present, but with much less intensity. The dominance of the LMB peak in the direct ion spectrum is striking given that the organic portion of MB is cationic and all that is required to obtain it in the mass spectrum is to dissociate it from the Cl^- ion. LMB also dominates the direct ion spectra of MB on gold and titanium metal surfaces, indicating that it is not the product of a surface reaction specific to nc-TiO_2. Whether LMB is present initially or is produced during the desorption event is unclear.

Comparison of the SIMS and laser desorption direct ion spectra shows that the laser does not induce oxidation reactions on the surface even though the photon energy (3.49 eV) is above the band gap of TiO_2 (3.2 eV). To test whether this was due merely to a lack of oxygen at the surface (typical chamber pressure = 2×10^{-9} mbar), the chamber was backfilled with oxygen to a partial pressure of 2.5×10^{-7} mbar and the laser was left to irradiate the film for 60 min at 500 Hz at a power just below the desorption threshold (∼5×10^6 W/cm^2). This corresponds to an oxygen arrival rate of 0.25 monolayer/s, or 900 monolayers/h, and a UV dose of ∼7×10^4 J/cm^2 over the course of the irradiation. The test area of the film was analyzed via 15 kV Ga^+ SIMS before and after irradiation. No changes were observed even though the integrated UV dose was several orders of magnitude higher than that required to cause pronounced changes in the spectrum when the exposure was done with an arc lamp in air (see below).

While direct ion mass spectra of MB on nc-TiO_2 can be obtained quite easily as shown in Fig. 3, the spectra exhibit a pronounced dependence on the power of the desorption laser. Generally, increasing the laser power increases the signal levels, but above a certain level fragmentation dominates to the extent that the MB parent ions all but vanish at high laser powers. The intensities of Ti and of some typical surface species (like Na and K) strongly increase and approach saturation as the laser power is increased. Fig. 4 shows the laser power dependence for some selected atomic and molecular ions desorbed from a MB-covered nc-TiO_2 surface. To ensure high and stable signals for the MB parent ion with as little fragmentation as possible, a laser power in an intermediate range (10–20 μJ/pulse, ∼1–2×10^7 W/cm^2) was employed for the laser desorption experiments.

The mass spectrum of MB laser desorbed from nc-TiO_2 and photoionized with a F_2 laser (Fig. 5) was similar to the direct ion spectrum shown in Fig. 3. The base peak is again $[LMB]^+$, however the main fragment peak corresponding to Azure B is found at $[M-1]^+$ rather than $[M+1]^+$. This is likely due to loss of a methyl group from MB, which results in a neutral molecule which is then ionized by the F_2 laser. The mass spectrum of Ar^+-sputtered neutrals photoionized with the F_2 laser is identical to the SIMS spectrum shown in Fig. 1. Examining the neutral channel via post-ionization for both ion and laser desorption demonstrated that the direct ion channel was an accurate reflection of the composition of the surface constituents for the MB/nc-TiO_2 system (at least qualitatively). This is an important observation, since the ionic and neutral channels of desorption are not often similar. Since neutral channel analysis is significantly more complicated than measuring the direct ion channel and because no additional information was revealed from post-ionized neutral analysis, the majority of the data was obtained with direct ion measurements once the fact that the neutral and ion channels track each other was proven.

3.2. TiO_2 films with methylene blue upon UV irradiation

UV exposure of the MB-covered nc-TiO_2 films in air produced distinct changes in the visual appearance and mass spectra of the samples. The MB-treated films were initially

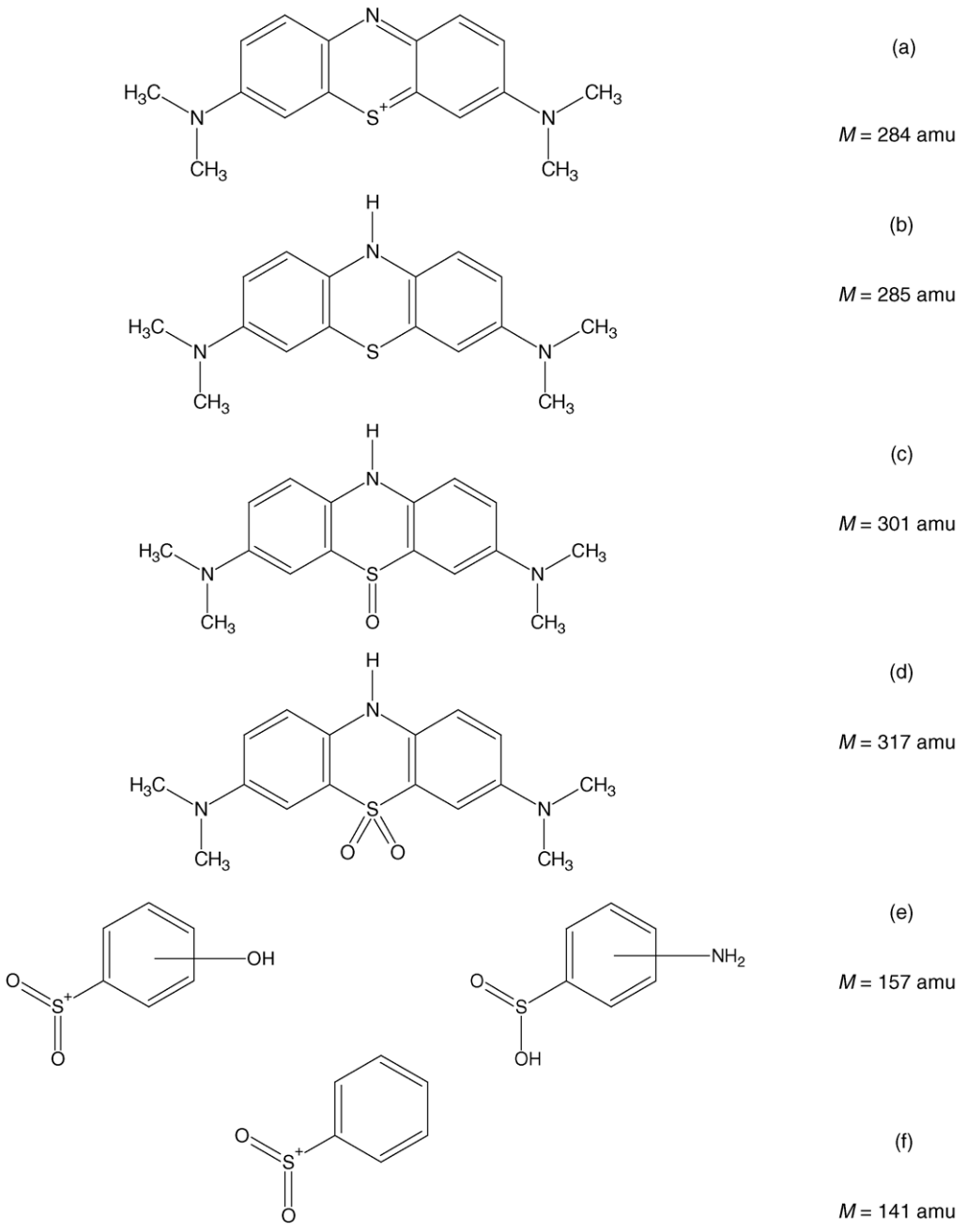

Fig. 2. Some of the molecules detected in the mass spectra: (a) methylene blue cation, $m/z = 284$ amu, (b) leucomethylene blue, $m/z = 285$ amu, (c) the leucomethylene blue sulfoxide, $m/z = 301$ amu, (d) the leucomethylene blue sulfone, $m/z = 317$ amu, and proposed structures for ions at $m/z = 157$ amu (e) and $m/z = 141$ amu (f).

dark blue or violet; upon brief UV exposure they turned to a light blue and were almost white after long exposures. These color changes correlate with changes in the mass spectra. Fig. 6 shows direct ion spectrum of a specimen exposed to UV light for 5 min at a power density of 6.4 mW/cm^2. The parent ion (LMB) and the Azure B fragment have nearly vanished, and the dominant high-mass peaks are at $m/z = 301$ and 317. These are likely due to oxidation of the parent molecule. Similar species have been reported in recent work [23] on photocatalytic degradation of MB in an aqueous suspension of 30 nm TiO_2 particles. There, it was proposed that OH radicals attack the C–S^+ = C functional group of MB, which at low pH is in direct Coulombic interaction with the anionic TiO_2 surface. It was further argued that the first step in MB degradation is oxygen addition to the C–S^+ = C functional group. The resulting sulfoxide, which had also undergone a ring-opening reaction at the N heteroatom, was detected at $m/z = 303$ amu by GC/MS. This ring-opening can occur when the attack takes place on the MB cation with the charge concentrated on the sulfur atom, however if neutral LMB

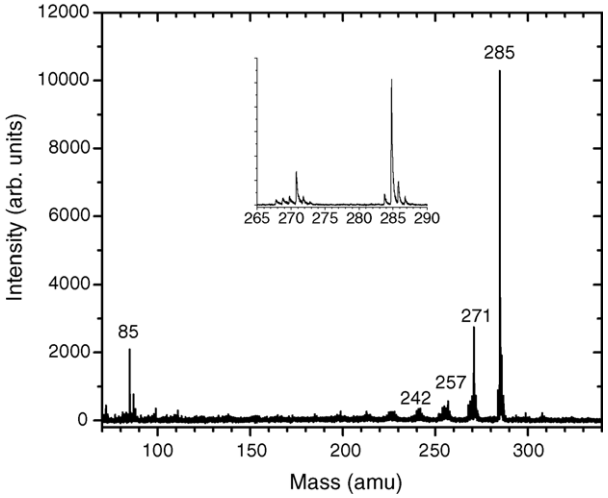

Fig. 3. Laser desorption direct ion mass spectrum (λ = 355 nm) of methylene blue on a nc-TiO_2 film.

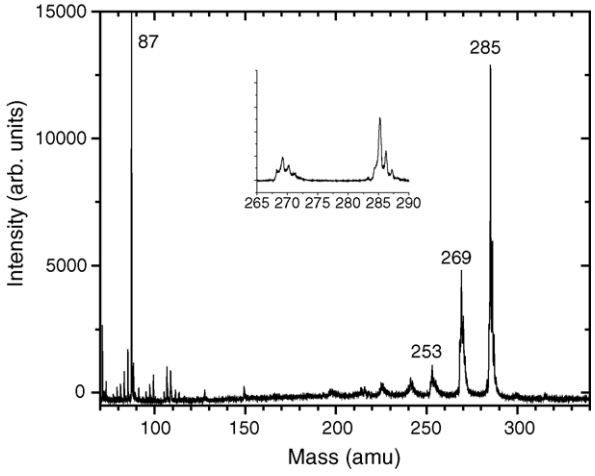

Fig. 5. Mass spectrum obtained by laser desorption (λ = 337 nm) and photoionization (λ = 157 nm) of neutral species from a nc-TiO_2 film covered by methylene blue.

is attacked or if the cationic sulfur is coordinated by TiO_2 surface oxygen, no such ring-opening is required and the sulfoxide has structure *c* in Fig. 2 and is detected at $m/z = 301$.

The sulfoxide group can react with a second OH radical to produce a sulfone. This may proceed on LMB sulfoxide without disrupting the ring structure as shown in structure d in Fig. 2, which we detect at $m/z = 317$. Note that here the sulfur atom is in the maximally stable +6 oxidation state. In addition, oxidative dissociation of the central ring as described in ref. [23] can result in various sulfone-containing fragments. The sulfones were not detected in [23], but it is well known [41] that the sulfoxide is easily oxidized into the sulfone in the presence of hydroperoxides. The latter are thought to be formed, at least transiently, via the neutralization of O_2^- by protons, cf. Eqs. (5)–(7). Although these species cannot be monitored in the present experiment, recent thermal desorption mass spectrometry from pure TiO_2 films showed [37] the abundant desorption of O_2 and OH molecules at low temperature; that is, of weakly bound species. In the present experiment, two fragments representing sulfones are detected at $m/z = 157$ and 141, corresponding to structures e and f in Fig. 2. These species derive from dissociation of the central ring after sulfone formation, accompanied by loss of a dimethylamino group. They may be fragments produced by laser irradiation of the LMB sulfone, or may be the products of reactions on the nc-TiO_2 surface. We favor the later interpretation since we do not see laser-generated fragments corresponding to LMB sulfone that has lost one or both of its dimethylamino groups. These would have appeared at $m/z = 274$ and 231 in Fig. 3.

The UV dose required to bring about these changes was ~2 J/cm^2, or roughly a factor of 10^4 lower than the dose delivered by the laser in the earlier experiment in which the mass

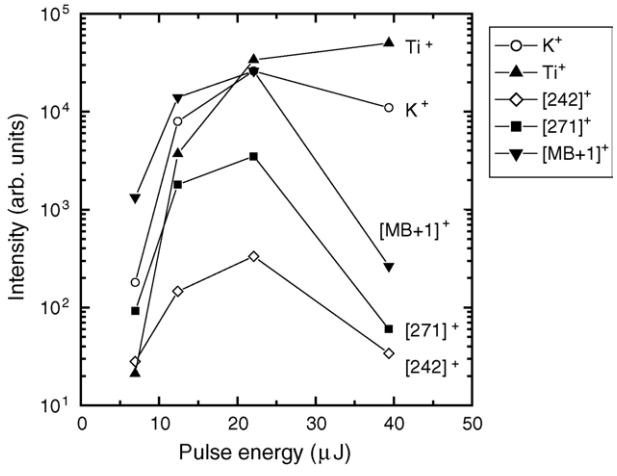

Fig. 4. Intensity of various atomic and molecular ions laser desorbed from a nc-TiO_2 film covered by methylene blue as a function of the laser pulse energy. Apart from K^+ (◯) and Ti^+ (▲), the methylene blue parent ion, $[MB+1]^+$ (▼) and two fragment species at $m/z = 242$ (◊) and 271 (■) are shown.

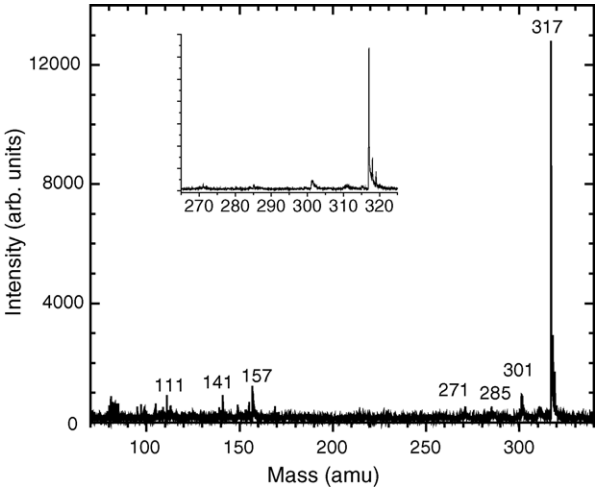

Fig. 6. Laser desorption direct ion mass spectrum (λ = 355 nm) of methylene blue on a nc-TiO_2 film after UV irradiation for 5 min at 6.4 mW/cm^2.

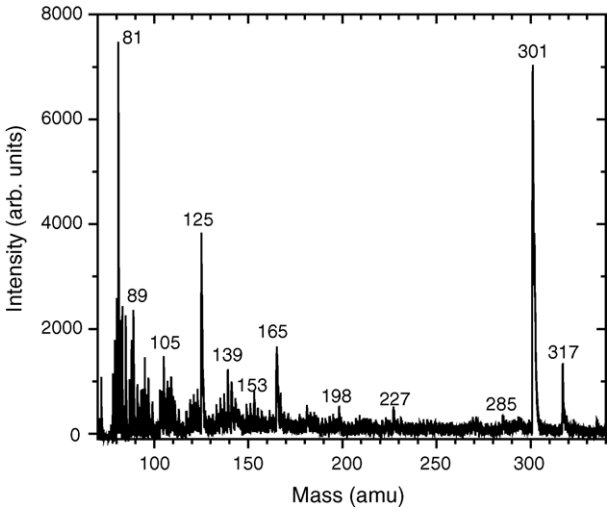

Fig. 7. Laser desorption direct ion mass spectrum (λ = 355 nm) of methylene blue on a nc-TiO_2 film after UV irradiation for 1 min at 1 W/cm^2.

spectrometer chamber was backfilled with oxygen. Given that no reaction was observed under high vacuum conditions or with only oxygen present, this implicates the water-derived OH radical in the reaction mechanism (e.g., reactions (2), (4), and (8)) rather than molecular oxygen or direct oxidation by holes (reactions (3) and (9)).

For more intense UV exposures the MB parent ion and the Azure B fragment vanish completely. The spectrum of Fig. 7 was taken from a specimen irradiated for 1 min at a power density of 1 W/cm^2 (integrated UV dose ∼60 J/cm^2), and shows the LMB sulfoxide and sulfone peaks, though their relative intensities are reversed. Most of the other peaks originate from the underlying TiO_2 film, as can be inferred from a comparison with Fig. 8, which is a spectrum of an untreated nc-TiO_2 film taken under the same conditions as Fig. 7 but without the UV exposure. In particular, the peaks at the m/z = 81, 105, 125, 139, 153, 165, 181, and 198 amu are

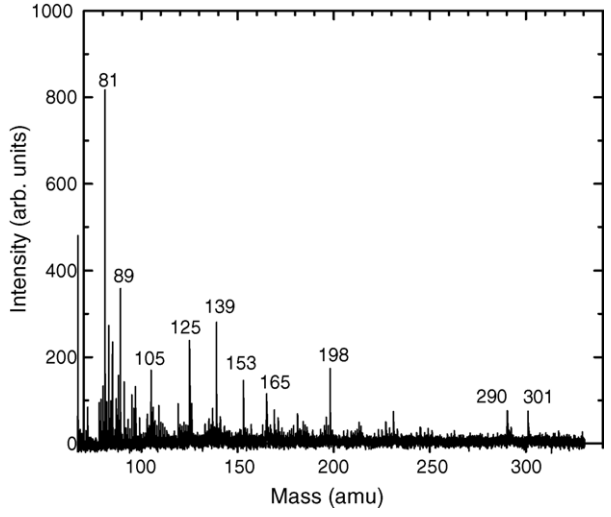

Fig. 8. Laser desorption direct ion mass spectrum (λ = 355 nm) of a pristine nc-TiO_2 film.

observed in both spectra. The relative peak heights between Figs. 7 and 8 are not indicative of the relative amounts of material present because the laser intensities were not the same (12 μJ for Fig. 7 versus 26 μJ for Fig. 8). Nevertheless it is clear that there is much less organic material present on the sample after the high-intensity UV exposure. This is corroborated by a visual inspection of the sample, which shows it to be essentially white. We may conclude, therefore, that an appreciable amount of the methylene blue has been mineralized at the nc-TiO_2 surface upon UV irradiation. Because of their volatile nature, the final mineralization products (e.g., CO_2, SO_4, NH_4, and NO_3) could not be detected in this experiment; however, the identification of some reaction intermediates by surface mass spectrometry appears to open an interesting avenue for further studies of photocatalytic reactions on nc-TiO_2 films.

4. Conclusions

Photodegradation reactions of methylene blue on nanocrystalline TiO_2 films can be studied in situ using mass spectrometric techniques that analyze material desorbed from the sample surface. Among the methods studied here, laser desorption direct ion mass spectrometry proved to be a facile technique that reveals several reaction intermediates with little fragmentation, and without the laser probe itself affecting the reaction. It was shown for the MB/nc-TiO_2 system that the neutral and ion species observed are qualitatively similar. The first products in the oxidation process induced by UV exposure in air revealed by this method are the sulfoxide and sulfone of leucomethylene blue, the reduced form of methylene blue.

Acknowledgements

We are grateful to A. Orendorz for providing the nanocrystalline TiO_2 films. One of the authors (H.G.) thanks Argonne National Laboratory for financial support. This work was supported by the U.S. Department of Energy, BES-Materials Sciences, under Contract W-31-109-ENG-38.

References

[1] M.A. Fox, M.T. Dulay, Chem. Rev. 93 (1993) 341.
[2] M. Anpo, M. Takeuchi, J. Catal. 216 (2003) 503.
[3] A. Hagfeldt, M. Grätzel, Chem. Rev. 95 (1995) 49.
[4] M. Grätzel, Nature 414 (2001) 338.
[5] L.R. Skubal, N.K. Meshkov, M.C. Vogt, J. Photochem. Photobiol. A: Chem. 148 (2002) 103.
[6] A. Mills, S. LeHunte, J. Photochem. Photobiol. A: Chem. 108 (1997) 1.
[7] A. Fujishima, T.N. Rao, D.A. Tryk, J. Photochem. Photobiol. C: Photochem. Rev. 1 (2000) 1.
[8] H. Gnaser, B. Huber, C. Ziegler, in: H.S. Nalwa (Ed.), Encyclopedia of Nanoscience and Nanotechnology, vol. 6, American Scientific Publishers, Stevenson Ranch, 2004, p. 505.

[9] M. Schiavello (Ed.), Photocatalysis and Environment, Kluwer Academic Publishers, Dordrecht, 1988.
[10] D.F. Ollis, H. Al-Ekabi (Eds.), Photocatalytic Purification and Treatment of Water and Air, Elsevier, Amsterdam, 1993.
[11] P.V. Kamat, Chem. Rev. 93 (1993) 267.
[12] A. Heller, Acc. Chem. Res. 28 (1995) 503.
[13] J. Peral, X. Domènech, D.F. Ollis, J. Chem. Technol. Biotechnol. 70 (1997) 117.
[14] A.L. Linsebigler, G. Lu, J.T. Yates Jr., Chem. Rev. 95 (1995) 735.
[15] M.R. Hoffmann, S.T. Martin, W. Choi, D.W. Bahnemann, Chem. Rev. 95 (1995) 69.
[16] P.V. Kamat, in: J.H. Fendler (Ed.), Nanoparticles and Nanostructured Films, Wiley-VCH, Weinheim, 1998, p. 207.
[17] A. Mills, G. Hill, S. Bhopal, I.P. Parkin, S.A. O'Neill, J. Photochem. Photobiol. A: Chem. 160 (2003) 185.
[18] J.C. Vickerman, D. Briggs (Eds.), TOF-SIMS: Surface Ananysis by Mass Spectrometry, IM Publications, Chichester, 2001.
[19] H. Zollinger (Ed.), Color Chemistry. Synthesis, Properties and Applications of Organic Dyes and Pigments, second ed., VCH, Weinheim, 1991.
[20] R.W. Matthews, J. Chem. Soc., Faraday Trans. 85 (1989) 1291.
[21] S. Lakshmi, R. Renganathan, S. Fujita, J. Photochem. Photobiol. A: Chem. 188 (1995) 163.
[22] T. Zhang, T. Oyama, A. Aoshima, H. Hidaka, J. Zhao, N. Serpone, J. Photochem. Photobiol. A: Chem. 140 (2001) 163.
[23] A. Houas, H. Lachheb, M. Ksibi, E. Elaloui, C. Guillard, J.-M. Herrmann, Appl. Catal. B: Environ. 31 (2001) 145.
[24] H. Lachheb, E. Puzenat, A. Houas, M. Ksibi, E. Elaloui, C. Guillard, J.-M. Herrmann, Appl. Catal. B: Environ. 39 (2002) 75.
[25] G. Liu, T. Wu, J. Zhao, H. Hidaka, N. Serpone, Environ. Sci. Technol. 33 (1999) 2081.
[26] C. Galindo, P. Jacques, A. Kalt, J. Photochem. Photobiol. A: Chem. 130 (2000) 35.
[27] M. Vautier, C. Guillard, J.-M. Herrmann, J. Catal. 201 (2001) 46.
[28] J. Grzechulska, A.W. Morawski, Appl. Catal. B: Environ. 36 (2002) 45.
[29] J. Li, C. Chen, J. Zhao, H. Zhu, J. Orthman, Appl. Catal. B: Environ. 37 (2002) 331.
[30] Z. Sun, Y. Chen, Q. Ke, Y. Yang, J. Yuan, J. Photochem. Photobiol. A: Chem. 149 (2002) 169.
[31] M. Sökmen, A. Özkan, J. Photochem. Photobiol. A: Chem. 147 (2002) 77.
[32] S. Sakthivel, M.V. Shankar, M. Palanichamy, B. Arabindoo, V. Murugesan, J. Photochem. Photobiol. A: Chem. 148 (2002) 153.
[33] S. Al-Qaradawi, S.R. Salman, J. Photochem. Photobiol. A: Chem. 148 (2002) 161.
[34] T. Sauer, G. Cesconeto Neto, H.J. José, R.F.P.M. Moreira, J. Photochem. Photobiol. A: Chem. 149 (2002) 147.
[35] J.-M. Wu, T.-W. Zhang, J. Photochem. Photobiol. A: Chem. 162 (2004) 171.
[36] B. Huber, H. Gnaser, C. Ziegler, Anal. Bioanal. Chem. 375 (2003) 917.
[37] B. Huber, A. Brodyanski, M. Scheib, A. Orendorz, C. Ziegler, H. Gnaser, Thin Solid Films 472 (2005) 114.
[38] Z. Ma, R.N. Thompson, K.R. Lykke, M.J. Pellin, A.M. Davis, Rev. Sci. Instrum. 66 (1995) 3168.
[39] M.R. Savina, M.J. Pellin, C.E. Tripa, I.V. Veryovkin, W.F. Calaway, A.M. Davis, Geochim. Cosmochim. Acta 67 (2003) 3215.
[40] I.V. Veryovkin, W.F. Calaway, J.F. Moore, M.J. Pellin, D.S. Burnett, Nucl. Instrum. Methods B219-B220 (2004) 473.
[41] H. Beyer, W. Walter, Lehrbuch der Organischen Chemie, Hirzel Verlag, Stuttgart, 1998.